Supporting Information

$CoCr_2O_4$ Nanospheres for Low Temperature Methane Oxidation

Yiling Dai,[a] Haiyan Wang, [b] Shida Liu, [b] Kevin J. Smith,*[b] Michael O. Wolf,*[a] and Mark J. MacLachlan*[a]

Table S1. Yields of $CoCr_2O_4$ prepared with different solvothermal reaction times.

Solvothermal reaction time for $CoCr_2O_4$	Yield after solvothermal reaction (g)	Yield after calcination (g)
1 h	0.6484	0.4196
3 h	0.6856	0.4224
6 h	0.7492	0.4324
8 h	0.7500	0.4466
12 h	0.7544	0.4473
24 h	0.6819	0.4360

Table S2. Yields of $CoCr_2O_4$ without adding benzyl alcohol.

Solvothermal reaction time for $CoCr_2O_4$	Yield after solvothermal reaction (g)	Yield after calcination (g)
Control-1h	0.6171	0.4152
Control-8h	0.6401	0.4228
Control-24h	0.5952	0.4067

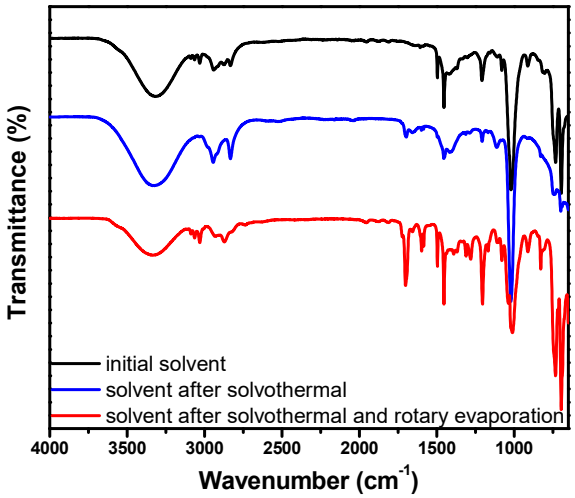

Fig. S1. FT-IR spectra for the solvent before and after solvothermal process.

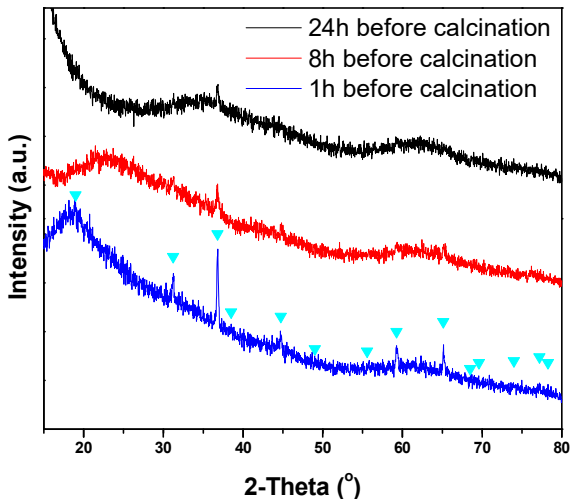

Fig. S2. PXRD patterns of $CoCr_2O_4$ precursor with different times of solvothermal treatment. (▼) Spinel, syn – $Co_{2.74}O_4$ (JCPDS 78-5614).

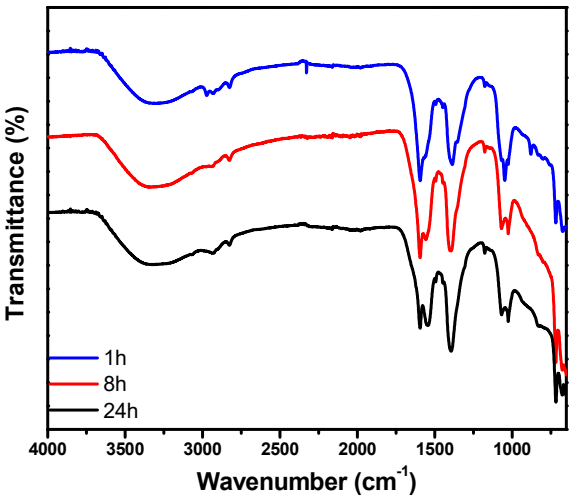

Fig. S3. FTIR spectra for $CoCr_2O_4$ precursors prepared with different solvothermal reaction times.

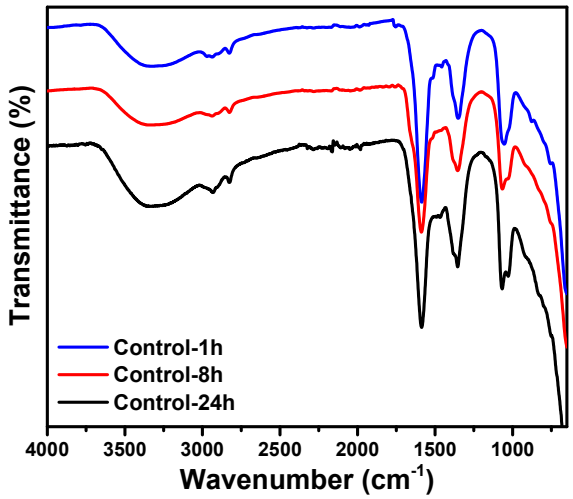

Fig. S4. FTIR spectra for $CoCr_2O_4$ precursors prepared with different solvothermal reaction times without adding benzyl alcohol. Strong peaks at 1586 and 1355 cm^{-1} are due to the asymmetric and symmetric C=O stretching of salts of carboxylic acids, respectively. Medium intensity bands at 2935 and 2823 cm^{-1} are assigned to the antisymmetric and symmetric stretching of CH_3. A strong band at 1031 cm^{-1} is due to C-O stretching.

Table S3. Weight percentage of different elements for $CoCr_2O_4$ precursor.

$CoCr_2O_4$ precursor	Co (wt %)	Cr (wt %)	C (wt %)	O (wt %)	H (wt %)
1h	9.1	15.9	33.0 (11.2)[a]	42.0	(3.1)
8h	14.1	25.7	28.9 (11.9)	31.3	(3.7)
24h	14.2	22.6	30.3 (12.8)	32.9	(3.4)
Control-1h	21.5	40.0	16.4	22.2	
Control-8h	22.3	39.7	16.1	22.0	
Control-24h	22.5	41.5	16.0 (5.0)	21.0	(3.7)

[a]Data in parentheses were determined by combustion elemental analysis. The difference in C analysis likely arises from the fact that XPS profiles a limited depth while combustion analysis gives a bulk analysis. The C analysis from combustion is most accurate for the bulk material; XPS is most useful for elemental ratios in the samples.

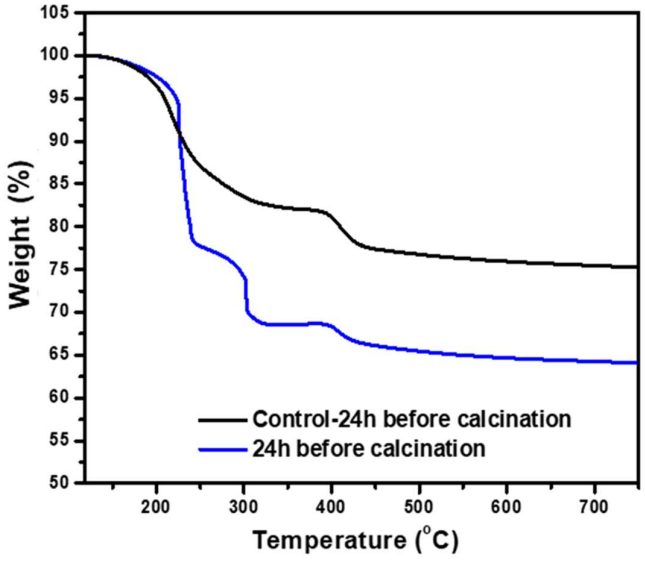

Fig. S5. TGA traces for the $CoCr_2O_4$ precursors prepared with or without adding benzyl alcohol during the solvothermal reaction.

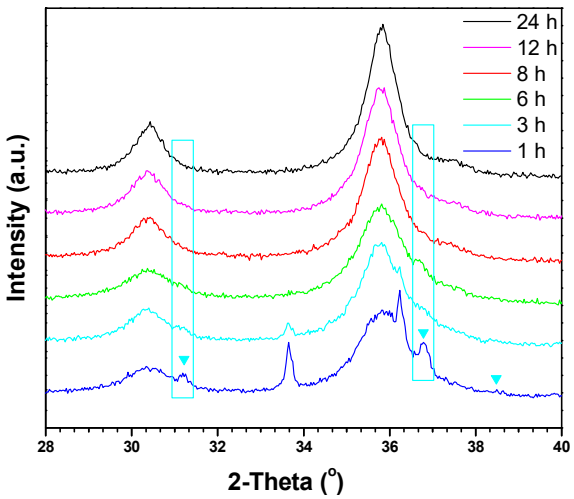

Fig. S6. PXRD patterns for $CoCr_2O_4$ prepared with different solvothermal reaction times. (▼) Spinel, syn – $Co_{2.74}O_4$ (JCPDS 78-5614).

Table S4. Particle size calculated with the Scherrer equation for $CoCr_2O_4$ catalysts.

Sample	Particle size determined from (220) (nm)	Particle size determined from (311) (nm)
6 h	7.0	6.1
8 h	8.6	7.2
12 h	9.0	7.5
24 h	10.4	8.4

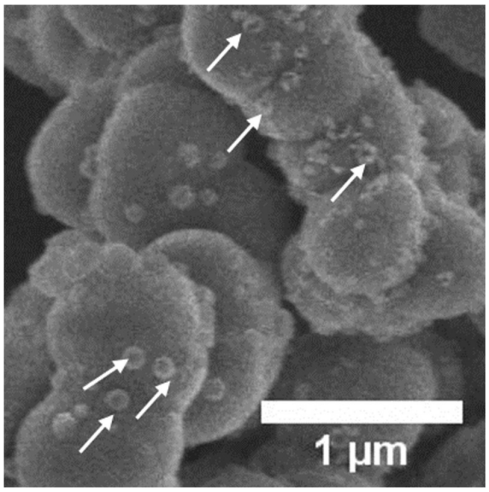

Fig. S7. SEM image for $CoCr_2O_4$ prepared with 8 h solvothermal treatment. The white arrows point to the hollow structure or breakage of Co_3O_4.

Table S5. Comparison of catalytic performance of $CoCr_2O_4$ for methane combustion with literature compositions.

Catalysts	GHSV (mL/(g•h))	$T_{10\%}$	$T_{50\%}$	$T_{90\%}$	reference
$CoCr_2O_4$ (8 h)	180,000	318	396	453	This work
$CoCr_2O_4$	36,000		392	464	[1]
$CoCr_2O_4$	48,000	500		750	[2]
$CoCr_2O_4$	36,000		420	514	[3]
$CoCr_{1.95}V_{0.05}O_4$	36,000		388	438	[3]
$LaFeAl_xO_y$(LF1A)	48,000	450	555	640	[4]
$LaCO_3OH/Co_3O_4$/graphene	10,000		315	420	[5]
Co_3O_4/Al_2O_3 (CC)	60,000	335	430	505	[6]
Ce/Co_3O_4	60,000	340	425	495	[6]
CoNi(50:50)	60,000			466	[7]
3DOM-m $La_{0.7}Ce_{0.3}CoO_3$	30,000	381	479	555	[8]

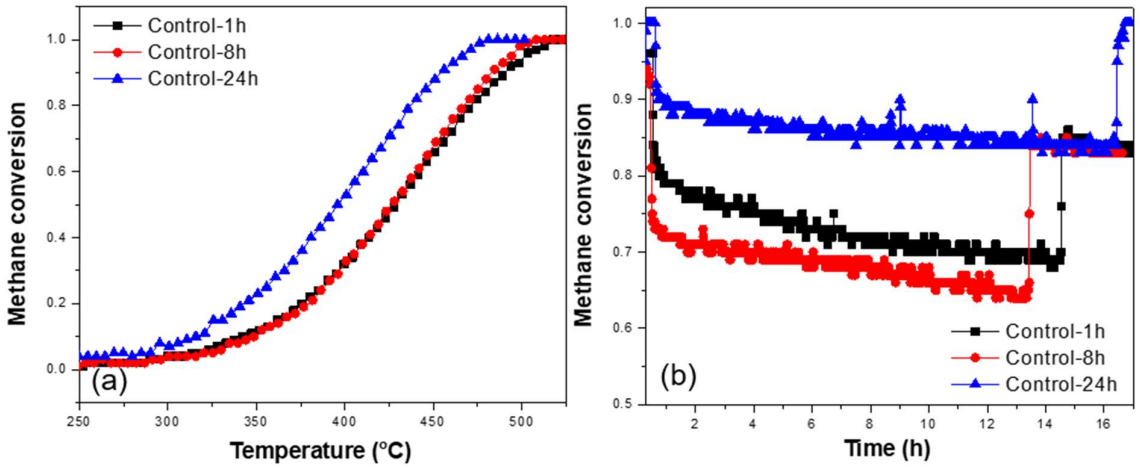

Fig. S8. Catalytic performance in dry (a) and wet (b) conditions for control $CoCr_2O_4$ samples prepared without benzyl alcohol.

Table S6. Comparison of stability for the $CoCr_2O_4$ catalysts prepared with and without adding benzyl alcohol.

$CoCr_2O_4$	Conversion drops at the beginning of H_2O and SO_2 injection	Conversion in the presence of SO_2 and H_2O within 13 h	Decreased conversion in total
24 h	98-80% (Δ = 18%)	80-78% (Δ = 2%)	20%
Control-24h	100-90% (Δ = 10%)	90-84% (Δ = 6%)	16%
8 h	100-92% (Δ = 8%)	92-88% (Δ = 4%)	12%
Control-8h	95-75% (Δ = 20%)	75-66% (Δ = 8%)	28%
1 h	-	99-85% (Δ = 14%)	14%
Control-1h	96-82% (Δ = 14%)	82-69% (Δ = 13%)	28%

Table S7. Comparison of stability for methane combustion with literature.

Catalysts	Conditions	Time (h)	Stability in feed gas	Reversibility ΔT (°C)[a]	reference
$CoCr_2O_4$ 8h	10% H_2O, 5 ppm SO_2 at 500 °C	170	100%-78%	30	This work
0.33Pt-0.67Pd /$MnLaAl_{11}O_{19}$	3% H_2O, 1000 ppm SO_2, 670 °C	10	100%-99%	60	9
	3% H_2O, 1000 ppm SO_2, 495 °C	5	93%-93%	-	
Pd-CeNW@SiO_2	5% H_2O, 20 ppm SO_2 at 450 °C	10	100%-100%	-	10
	5% H_2O, at 375 °C	24	100%-75%	-	
$PdPt/Al_2O_3$	5% H_2O, 10 ppm SO_2 at 500 °C	4	87%-10%	-	11
Cr_2O_3	Emission from a coke oven, with NH_3, N_2, H_2,	40	100%-90%	-	12
$La_{0.9}Ce_{0.1}CoO_3$	H_2O, CO, CO_2, SO_2 and H_2S at 450 °C	35	95%-75%	-	
$10Ce/Co_3O_4$	5% H_2O, at 450 °C	150	75%-40%	10	6
$LaCoO_3$	100 ppm SO_2 at 600 °C	3	-	60	13

[a] ΔT indicates the $T_{50\%}$ shift between fresh and used catalysts measured under dry conditions.

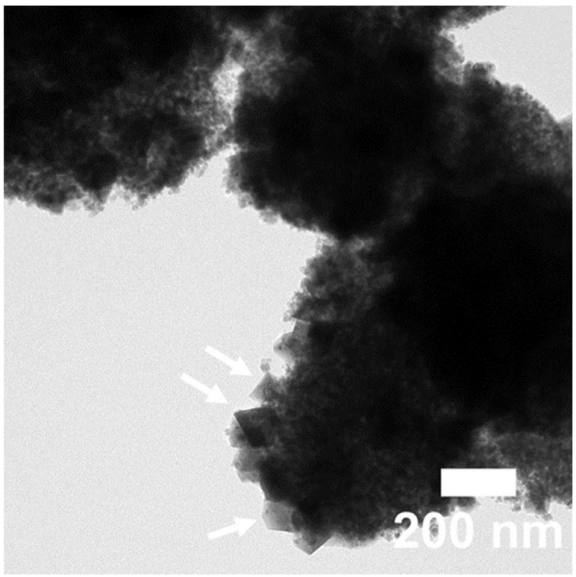

Fig. S9. TEM image for $CoCr_2O_4$ 8 h after durability test. The white arrows point to the sintered Co_3O_4 particles.

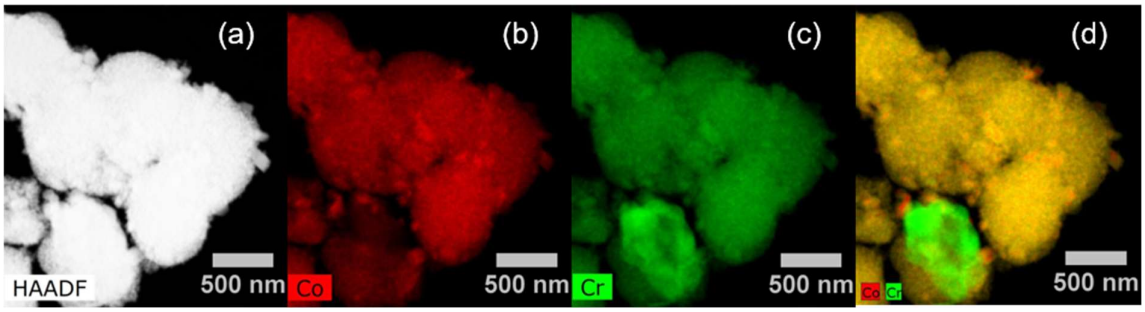

Fig. S10. EDX mapping for $CoCr_2O_4$ 8 h catalysts after durability test.

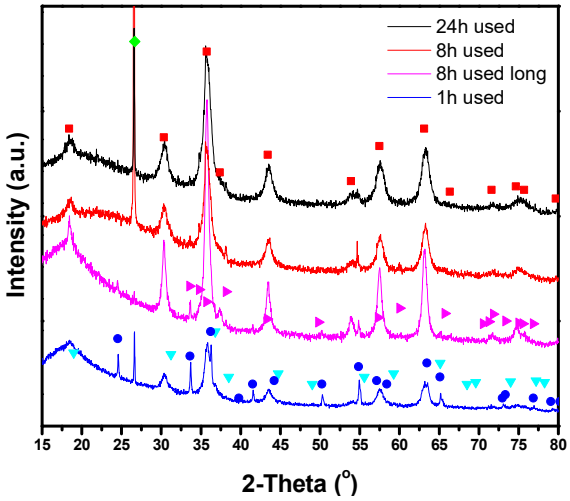

Fig. S11. PXRD patterns for used $CoCr_2O_4$ catalysts. (■) Cobalt chromite, syn – $CoCr_2O_4$ (JCPDS 22-1084). (▼) Spinel, syn – $Co_{2.74}O_4$ (JCPDS 78-5614). (●) Eskolaite, syn – Cr_2O_3 (JCPDS 38-1479). (♦) Quartz, syn – SiO_2 (JCPDS 79-1910). (►) Moissanite 4H – SiC (JCPDS 72-4532).

Table S8. Particle size calculated with the Scherrer equation for the fresh and used catalysts.

Sample	Particle size from (220) (nm)	Particle size from (311) (nm)
8h fresh	8.6	7.2
8h used	9.4	8.6
8h long used	14.7	11.8
24h fresh	10.4	8.4
24h used	10.6	8.7
Control-24h fresh	7.2	6.3
Control-24h used	7.5	6.7

Table S9. H_2-TPR profile and TOF for catalysts.

$CoCr_2O_4$	H_2 consumption T<250 °C (mmol/g (°C))	TOF (s^{-1})
$CoCr_2O_4$ 8h	0.39 (192)[a]	0.0090
$CoCr_2O_4$ Control-24h	0.42 (207)	0.0101
$CoCr_2O_4$ NH4OH	0.16 (180)	0.0077
$CoCr_2O_4$ NaOH	0.12 (171)	0.0041
Co_3O_4	0.62 (233)	0.0348
Cr_2O_3	0.18 (212)	0.0010

[a] Reduction temperature

Determination of Activation Energy

Previous research indicated that in oxidizing conditions, methane combustion follows a 1st order reaction mechanism with respect to methane. In this work, oxygen is in excess, so the reaction has a pseudo first-order reaction mechanism with respect to CH_4. So

$$r_{CH_4} = N_{CH_4} X \quad (1)$$

$$r_{CH_4} = \mathrm{k[CH_4]} = \left(\mathrm{A}\exp\left(-\frac{E_a}{RT}\right)\right)[\mathrm{CH_4}] \quad (2)$$

$$\ln r_{CH_4} = -\frac{1000E_a}{RT} + \ln A + \ln[\mathrm{CH_4}] \quad (3)$$

where r_{CH_4} is reaction rate (μmol/s), N_{CH_4} is methane flow rate (μmol/s), X is the conversion of methane, k is rate constant (s^{-1}), E_a is activation energy (kJ/mol), $[CH_4]$ is methane concentration (μmol) and A is pre-exponential factor.
The amount of methane is low, so $[CH_4]$ can be assumed to be approximately constant. E_a was obtained by the slope of the linear plot of $\ln r_{CH_4}$ versus 1000/T.

Additional Experimental Details

Chemicals

Cobalt(II) nitrate hexahydrate (Sigma-Aldrich, ≥ 98%), chromium(III) nitrate nonahydrate (Fisher Scientific, > 96%), cobalt(II) acetate tetrahydrate (Alfa Aesar, 98%), chromium(III) acetate hydrate (Matheson Coleman & Bell Manufacturing Chemists, Inc.), sodium hydroxide (Sigma-Aldrich, ≥ 97.0%), methanol (Sigma-Aldrich, ≥ 99.8%), benzyl alcohol (Sigma-Aldrich, ≥ 99%), ammonium hydroxide (Fisher Scientific, 28.0 to 30.0 w/w %) and other solvents were used without further purification.

Preparation of Co_3O_4 and Cr_2O_3 nanocrystals.

Cobalt(II) nitrate hexahydrate ($Co(NO_3)_2 \cdot 6H_2O$, 1.749 g, 6.000 mmol) or chromium(III) nitrate nonahydrate ($Cr(NO_3)_3 \cdot 9H_2O$, 2.401 g, 6.000 mmol) were dissolved in 20 mL methanol. Benzyl alcohol (3 mL, 29 mmol) was added and the solution was stirred for 1 h. The mixture was then transferred to a 45 mL Teflon-lined stainless steel autoclave. The sealed reaction vessel was heated at 180 °C for 8 h. After the reaction cooled to ambient conditions, the autoclave contents were collected by suction filtration. The dark green product was washed with ethanol three times, then dried at 100 °C for 2 h and calcined at 500 °C for 3 h.

Preparation of $CoCr_2O_4$ by the co-precipitation method with NaOH

Cobalt(II) acetate tetrahydrate ($Co(CH_3CO_2)_2 \cdot 4H_2O$, 0.8303 g, 3.333 mmol) and chromium(III) acetate hydrate ($Cr(CH_3CO_2)_3 \cdot H_2O$, 4.022 g, 6.667 mmol) were dissolved in 40 mL deionized water at 70 °C while stirring. A sodium hydroxide solution (prepared by dissolving 1.067 g NaOH in 10 mL H_2O) was added to the metal salt solution dropwise and the mixture continued stirring for 1 h at 70 °C. Afterward, the precipitate was collected by filtration, washed with H_2O and dried in an oven at 100 °C for 8 h. Finally, the product was calcined at 500 °C for 3 h.

Preparation of $CoCr_2O_4$ by the co-precipitation method with NH_4OH

Cobalt(II) nitrate hexahydrate ($Co(NO_3)_2 \cdot 6H_2O$, 0.7276 g, 2.500 mmol) and chromium(III) nitrate nonahydrate ($Cr(NO_3)_3 \cdot 9H_2O$, 2.001 g, 5.000 mmol) were dissolved in 30 mL deionized water. 10 wt % NH_4OH solution (10 mL NH_4OH diluted with 20 mL H_2O) was added to the above metal salt solution dropwise until the pH equaled to 9, then the mixture was stirred for 1 h. The precipitate was obtained by filtration, washed with H_2O and dried in oven at 100 °C for 8 h. Finally, the product was calcined at 500 °C for 3 h.

References

1. J. Chen, X. Zhang, H. Arandiyan, Y. Peng, H. Chang and J. Li, *Catal. Today*, 2013, **201**, 12.
2. J. Hu, W. Zhao, R. Hu, G. Chang, C. Li and L. Wang, *Mater. Res. Bull.*, 2014, **57**, 268.
3. J. H. Chen, W. B. Shi, S. J. Yang, H. Arandiyan and J. H. Li, *J. Phys. Chem. C*, 2011, **115**, 17400.
4. F. Huang, X. D. Wang, A. Q. Wang, J. M. Xu and T. Zhang, *Catal. Sci. Technol.*, 2016, **6**, 4962.
5. J. Li, M. Li, P. Gui, L. Zheng, J. Liang and G. Xue, *Catal. Today*, 2019, **327**, 134.
6. A. Choya, B. de Rivas, J. R. González-Velasco, J. I. Gutiérrez-Ortiz and R. López-Fonseca, *Appl. Catal., B*, 2018, **237**, 844.
7. T. H. Lim, S. J. Cho, H. S. Yang, M. H. Engelhard and D. H. Kim, *Appl. Catal., A*, 2015, **505**, 62.
8. H. Arandiyan, J. Scott, Y. Wang, H. Dai, H. Sun and R. Amal, *ACS Appl. Mater. Interfaces*, 2016, **8**, 2457.
9. S. A. Yashnik, Y. A. Chesalov, A. V. Ishchenko, V. V. Kaichev and Z. R. Ismagilov, *Appl. Catal., B*, 2017, **204**, 89.
10. H. Peng, C. Rao, N. Zhang, X. Wang, W. Liu, W. Mao, L. Han, P. Zhang and S. Dai, *Angew. Chem. Int. Ed.*, 2018, **57**, 8953.
11. N. Sadokhina, G. Smedler, U. Nylén, M. Olofsson and L. Olsson, *Appl. Catal., B*, 2018, **236**, 384.
12. S. Ordóñez, J. R. Paredes and F. V. Díez, *Appl. Catal., A*, 2008, **341**, 174.
13. G. S. Guo, K. Lian, L. J. Wang, F. B. Gu, D. M. Han and Z. H. Wang, *RSC Adv.*, 2014, **4**, 58699.

